Report

Neuron

Cocaine Place Conditioning Strengthens Location-Specific Hippocampal Coupling to the Nucleus Accumbens

Highlights

- Cocaine place conditioning increases subsequent firing in D2R medium spiny neurons
- Accumbens neurons decode spatial information from hippocampal inputs
- Increased accumbens firing is due to location-selective coupling with hippocampus

Authors

Lucas Sjulson, Adrien Peyrache, Andrea Cumpelik, Daniela Cassataro, György Buzsáki

Correspondence

luke@sjulsonlab.org (L.S.), gyorgy.buzsaki@nyumc.org (G.B.)

In Brief

Sjulson et al. demonstrate that cocaine place conditioning recruits location-dependent firing of medium spiny neurons in the nucleus accumbens. This recruitment is mediated primarily through selective coupling with hippocampal inputs that encode the cocaine-paired location, providing a possible substrate for storage of drug-location associations.

Sjulson et al., 2018, Neuron *98*, 1–9
June 6, 2018
https://doi.org/10.1016/j.neuron.2018.04.015

CellPress

Please cite this article in press as: Sjulson et al., Cocaine Place Conditioning Strengthens Location-Specific Hippocampal Coupling to the Nucleus Accumbens, Neuron (2018), https://doi.org/10.1016/j.neuron.2018.04.015

Neuron
Report

Cocaine Place Conditioning Strengthens Location-Specific Hippocampal Coupling to the Nucleus Accumbens

Lucas Sjulson,[1,2,4,*] Adrien Peyrache,[3] Andrea Cumpelik,[2,4] Daniela Cassataro,[2,4] and György Buzsáki[2,5,*]
[1]Department of Psychiatry, New York University School of Medicine, New York, NY 10016, USA
[2]NYU Neuroscience Institute, NYU School of Medicine, New York, NY 10016, USA
[3]Montreal Neurological Institute, McGill University, Montreal, QC H3A 2B4, Canada
[4]Present address: Department of Psychiatry and Behavioral Sciences, Dominick P. Purpura Department of Neuroscience, Albert Einstein College of Medicine, Bronx, NY 10461, USA
[5]Lead Contact
*Correspondence: luke@sjulsonlab.org (L.S.), gyorgy.buzsaki@nyumc.org (G.B.)
https://doi.org/10.1016/j.neuron.2018.04.015

SUMMARY

Conditioned place preference (CPP) is a widely used model of addiction-related behavior whose underlying mechanisms are not understood. In this study, we used dual site silicon probe recordings in freely moving mice to examine interactions between the hippocampus and nucleus accumbens in cocaine CPP. We found that CPP was associated with recruitment of D2-positive nucleus accumbens medium spiny neurons to fire in the cocaine-paired location, and this recruitment was driven predominantly by selective strengthening of coupling with hippocampal place cells that encode the cocaine-paired location. These findings provide *in vivo* evidence suggesting that the synaptic potentiation in the accumbens caused by repeated cocaine administration preferentially affects inputs that were active at the time of drug exposure. This provides a potential physiological mechanism by which drug use becomes associated with specific environmental contexts.

INTRODUCTION

A key insight into addiction is that drug use becomes associated with the environmental context in which the drug was administered, and re-exposure to the associated context leads to cravings or drug-seeking behavior. A simple model of this association is cocaine-conditioned place preference (CPP), in which cocaine is repeatedly paired with a specific spatial location causing the animal to spend more time in that location during subsequent exploration. Despite its simplicity and relevance, the neural mechanisms of cocaine CPP are still not understood.

The hippocampus (HPC) is a brain structure essential for spatial navigation, and it contains "place cells" that fire selectively in specific spatial locations (Kim et al., 2012; O'Keefe, 1976) or contexts (Komorowski et al., 2013). The CA1 and subiculum regions of the HPC send a strong projection to the nucleus accumbens (NAc) (Phillipson and Griffiths, 1985), and simultaneous HPC-NAc recordings in rats suggest that these HPC inputs carry spatial information to the NAc (Lansink et al., 2008; Lansink et al., 2009; Tabuchi et al., 2000; van der Meer and Redish, 2011a). Anatomical disconnection experiments indicate that HPC-NAc interactions are necessary for CPP (Ito et al., 2008), and NAc MSNs increase their firing rate near reward sites (Lansink et al., 2008; Lavoie and Mizumori, 1994; Miyazaki et al., 1998; van der Meer et al., 2010), possibly representing the readout of a stored location-reward association. Cocaine conditioning potentiates HPC synapses onto NAc MSNs, as tested in *ex vivo* slices (Britt et al., 2012; MacAskill et al., 2014; Pascoli et al., 2014), providing a potential substrate for storing this association. However, the neuronal mechanisms are unclear.

One possibility is that cocaine does not potentiate all HPC synapses in the NAc uniformly, as is often tacitly assumed. Plasticity at corticostriatal synapses generally requires presynaptic activity (Calabresi et al., 1999), raising the possibility that cocaine may selectively strengthen the synapses that were most active at the time of drug exposure. We thus hypothesized that cocaine would preferentially strengthen NAc coupling with HPC place cells that encode the cocaine-paired location. To test this hypothesis, we performed simultaneous dual site silicon probe recordings in the HPC and NAc of mice in a cocaine CPP paradigm. Our findings indicate that cocaine conditioning recruits location-specific MSN firing and suggest that this activity is driven predominantly by preferential strengthening of hippocampal inputs that encode the cocaine-paired location.

RESULTS

Dual Site Silicon Probe Recording during Cocaine-Conditioned Place Preference

We measured interactions between posterior CA1 and the NAc in hippocampus-dependent cocaine CPP (Ito et al., 2008; Meyers et al., 2003) (Figure S2A) using simultaneous silicon probe recordings in both structures (n = 10 mice) (Figure 1A). We used established criteria to identify putative pyramidal cells (PYRs) (Barthó et al., 2004; McCormick et al., 1985) in the hippocampus (n = 561 PYRs) and medium spiny neurons (MSNs) and

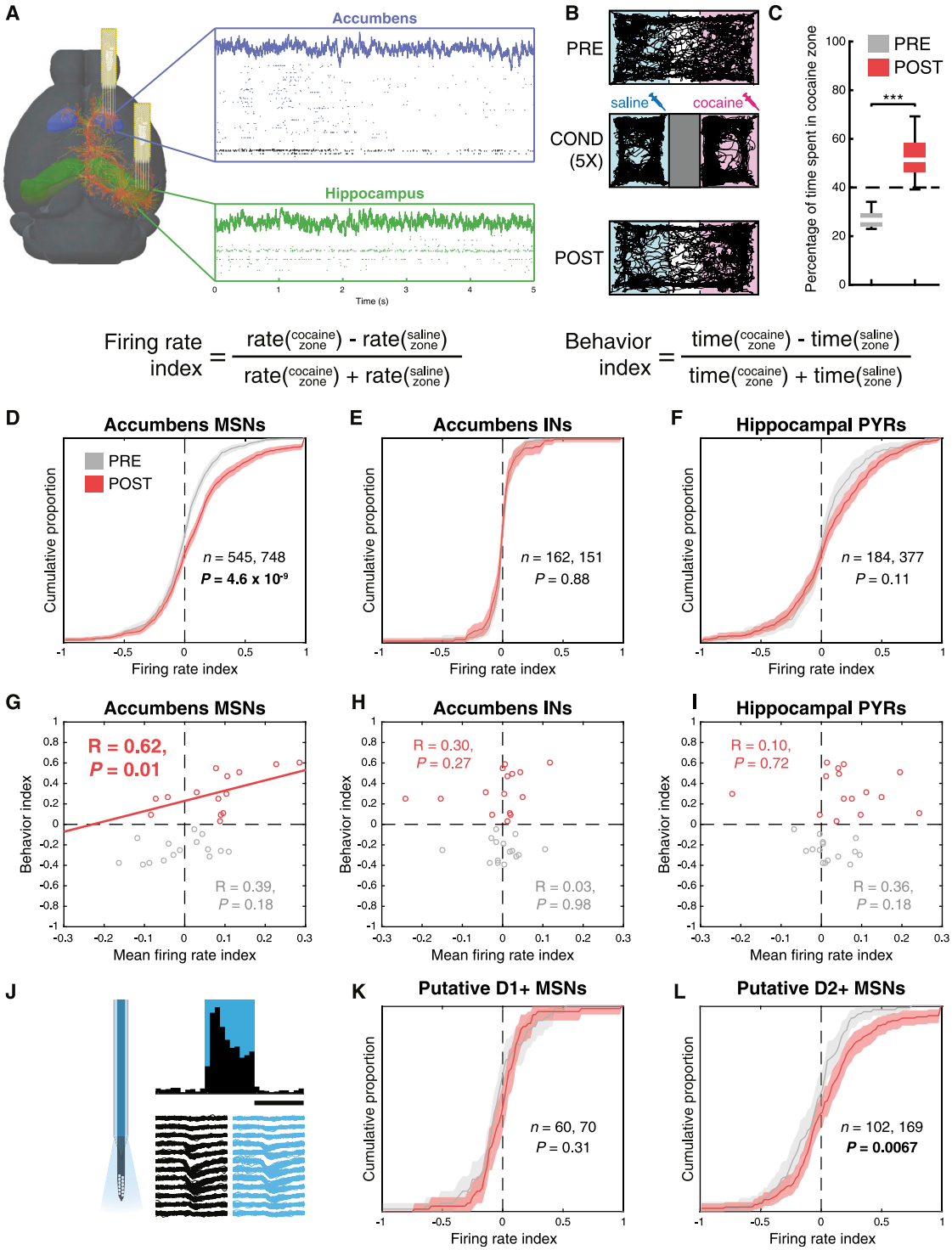

Figure 1. Cocaine Place Conditioning Increases Activity of D2-Positive MSNs in the Cocaine Zone

(A) Silicon probes were implanted in the hippocampus (green) and accumbens (blue), yielding LFP and single unit recordings (n = 1,606 accumbens neurons, 725 hippocampal neurons).

(B) Mice (n = 10) were conditioned for 5 days with saline and cocaine 15 mg/kg IP.

(C) In POST sessions, animals exhibited a preference for the cocaine-paired zone (***$p < 10^{-5}$, rank sum test).

(D) Accumbens MSNs fire preferentially in the cocaine zone after cocaine conditioning (t test, $p = 4.6 \times 10^{-9}$). Shaded area represents 99% confidence intervals.

(E and F) Accumbens putative interneurons (INs) (E) and hippocampal pyramidal cells (PYRs) (F) exhibit no shift after cocaine conditioning.

(legend continued on next page)

interneurons (INs) in the NAc (n = 1,293 MSNs, 313 INs; Figure S1) (Schmitzer-Torbert and Redish, 2008; Yamin et al., 2013). Recordings were performed in drug-free sessions either before (PRE) and after (POST) animals underwent cocaine place conditioning in a rectangular arena with a removable barrier (Figure 1B, Figure S2A). This conditioning paradigm induced CPP in POST sessions (PRE = 27% in cocaine zone, POST = 51%, rank sum test, n = 12 PRE, 15 POST sessions, $p = 1.6 \times 10^{-6}$; Figure 1C, Table S1), which was attributable to an increase in the proportion of time spent immobile in the cocaine zone (Figure S2).

Cocaine Place Conditioning Recruits D2-Positive MSNs

In POST sessions, NAc MSNs fire more when the animal is in the cocaine zone than the saline zone (firing rate index = −0.009 ± 0.011 PRE, 0.094 ± 0.013 POST, n = 545, 748 MSNs, t test, $p = 4.6 \times 10^{-9}$; Figure 1D). In contrast, firing rates were not different for NAc INs (n = 162, 151 INs, t test, p = 0.88, Figure 1E) or hippocampal PYRs (n = 184, 377 PYRs, p = 0.11, Figure 1F). However, the density of PYR place fields was higher in the cocaine zone in POST sessions ($p = 2.6 \times 10^{-8}$, Figure S4A). Further, we found that strength of behavioral CPP expression in a given POST session is correlated with the extent of increased MSN firing in the cocaine zone during that session (n = 15 POST sessions, R = 0.62, p = 0.01, Figure 1G). This correlation was observed only in POST sessions and was not observed in NAc INs (R = 0.3, p = 0.27; Figure 1H) or PYRs (R = 0.1, p = 0.72; Figure 1I). Using established optotagging techniques (Stark et al., 2012), we found that D2-positive MSNs were selectively recruited to the cocaine zone (Figures 1J–1L).

MSNs Entrained by Hippocampal Theta Encode More Spatial Information and Show Greater Recruitment by Cocaine Conditioning

Because MSN firing is strongly modulated by running speed (data not shown), and CPP results in correlations between location and running speed, (Figure S2), we used generalized linear models (GLMs) with model cross-validation to separate the different sources of variance in our observations. We found that the best model fit included separate terms for location and speed modulation (Table S2). This enabled us to dissociate speed and location and determine that MSNs exhibit running speed modulation that is independent of location and stronger than PYRs (n = 1,293 MSNs, 561 PYRs, rank sum test, $p = 3.9 \times 10^{-18}$) or NAc INs (Figure S3A, n = 561 PYRs, 313 INs, rank sum test, $p = 3.0 \times 10^{-5}$). After speed correction, MSNs encoded approximately as much spatial information (Skaggs et al., 1993) as hippocampal PYRs (Figure 2A, n = 1,293 MSNs, 561 PYRs, rank sum test, p = 0.20) and significantly more than INs (n = 1,293 MSNs, 313 INs, $p = 1.1 \times 10^{-38}$). To test whether MSNs received spatial information from the hippocampus, we used GLMs to predict MSN activity from combinations of location and spiking activity of hippocampal neurons (Figure 2B). We found that the correlated component of HPC and MSN activity carries spatial information (see STAR Methods, Figure 2C, n = 1,203 MSNs, signed rank test, $p = 4.1 \times 10^{-11}$). Prediction quality was highest when HPC led NAc by a time lag of ~30 ms (Figure 2D), suggesting directional information transfer from HPC to NAc. A similar analysis found that MSNs also decode information about running speed independent of location (Figures S3B–S3D). To test whether MSNs strongly modulated by HPC have different firing properties, we quantified phase locking of MSN firing to the HPC theta rhythm (Jones and Wilson, 2005; Lansink et al., 2009; Tabuchi et al., 2000; van der Meer and Redish, 2011a), using the parameter kappa of the Von Mises distribution (see STAR Methods; Figure 2E). We found that high kappa MSNs (strong phase locking) encode more spatial information (Figure 2F; 0.014 ± 0.005 versus 0.008 ± 0.003 bits/spike, rank sum test, $p = 3.9 \times 10^{-3}$) and exhibit larger recruitment to the cocaine zone than low kappa MSNs (Figures 2G and 2H; high kappa: PRE 0.0082 ± 0.013, POST 0.087 ± 0.017, n = 261, 351 MSNs; t test, $p = 2.7 \times 10^{-4}$; low kappa: PRE 0.0027 ± 0.016, POST 0.014 ± 0.016, n = 261, 351 MSNs; t test, p = 0.43).

Assembly Prediction Analysis Reveals Increased Hippocampus-Accumbens Coupling after Cocaine Conditioning

We next addressed the question of whether cocaine conditioning strengthens coupling between hippocampus and accumbens. We performed an assembly prediction analysis using PYR assemblies to predict the activity of a single MSN assembly (Figure 3A, STAR Methods). Consistent with our hypothesis that MSNs decode spatial information from hippocampal inputs, we found that the quality of the assembly prediction was correlated with the rate of spatial information encoded by the MSN assembly in POST, but not PRE, sessions (Figure 3B). The overall spatial information rate was also higher in POST sessions (Figure 3C, n = 34, 95 assemblies, rank sum test, $p < 0.05$), suggesting that cocaine conditioning strengthens hippocampus-accumbens coupling.

To ensure that our assembly prediction findings were not due to environmental cues or common inputs driving the HPC and NAc, we performed an analysis of sleep replay events. Replay events, which occur during HPC sharp-wave ripple oscillations, consist of temporally compressed firing of place cell sequences that encode recently visited spatial locations (Lee and Wilson, 2002; Nádasdy et al., 1999; Skaggs and McNaughton, 1996) and are generated locally in the hippocampus (Buzsáki et al., 1983). We used data from awake exploration of the CPP arena to fit the prediction weights of the GLM, then tested model predictions both on awake data withheld from the training set and on data collected during sleep ripples occurring before and after the animal explored the CPP arena. We found that

(G) Strength of behavioral CPP expression in each recording session is correlated with firing rate index in MSNs in POST (R = 0.62, p = 0.01, permutation test) but not PRE (p = 0.18) conditions.

(H and I) Behavioral CPP expression is not correlated with firing rate index in INs (H) or hippocampal PYRs (I).

(J) Tapered optical fibers attached to the silicon probe enabled optogenetic tagging of putative D1+ and D2+ cells (scale bar: 50 ms).

(K and L) Putative D1+ MSNs (K) showed no additional firing in the cocaine zone (N = 60, 70; t test, p = 0.31), but putative D2+ MSNs (L) fired preferentially in the cocaine zone after conditioning (N = 102, 169 units; t test, p = 0.0067).

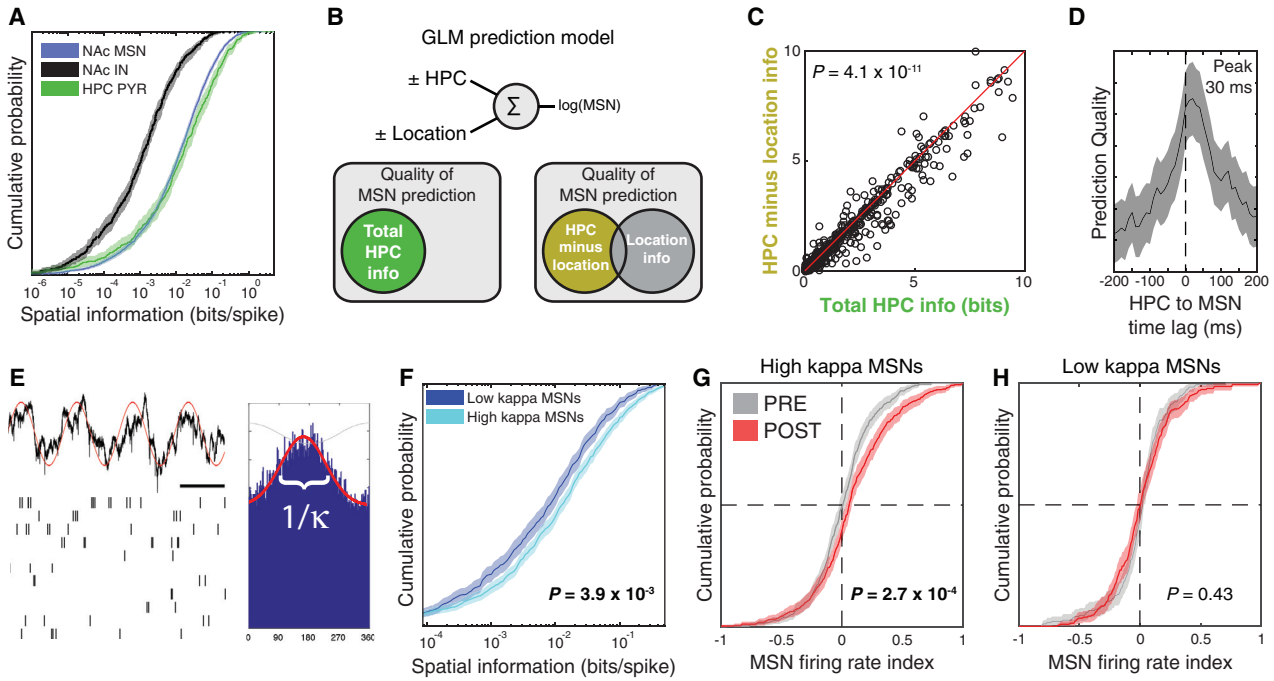

Figure 2. MSNs Receive Spatial Information from Hippocampus, and MSNs Phase Locked to the Hippocampal Theta Oscillation Encode More Spatial Information and Show Greater Recruitment by Cocaine Conditioning

(A) After correction for running speed, MSN and PYR activity carry similar amounts of spatial information ($p = 0.20$ for MSN versus PYR), but both contain more spatial information than IN activity (rank sum test, $p = 1.0 \times 10^{-38}$).

(B) GLMs enable prediction of individual MSN spike trains from the combination of PYR activity and location as predictors.

(C) Adding hippocampal activity as a predictor to a model already containing explicit location information results in a smaller improvement in prediction quality (signed rank test, $p = 4.1 \times 10^{-11}$) than for a model without explicit location information (note that most points are right of the diagonal). This suggests that predicting MSN spike trains from PYR inputs implicitly decodes information about spatial location.

(D) MSN spike train prediction quality is highest when PYR activity leads MSN activity by ~30 ms, supporting the hypothesis that information is transferred from PYRs to MSNs.

(E) The parameter K (kappa) quantifies phase locking of MSN spikes (bottom) to the hippocampal theta rhythm (top). Scale bar: 100 ms.

(F) High kappa MSNs (stronger phase locking) carry more spatial information than low kappa MSNs (rank sum test, $p = 3.9 \times 10^{-3}$).

(G and H) High kappa MSNs (G) exhibit increased activity in the cocaine zone after conditioning (t test, $p = 2.7 \times 10^{-4}$), but low kappa MSNS (H) do not (t test, $p = 0.43$). All shaded areas represent 99% confidence intervals.

during pre-exploration sleep, when replay events encoding locations in the CPP arena do not occur, the sleep ripple prediction quality was uncorrelated with wake prediction quality (Figure 3D). In contrast, during post-exploration sleep, the sleep ripple prediction quality was significantly correlated with wake prediction quality in POST sessions (Figure 3E), indicating strengthened hippocampus-NAc coupling.

Location-Specific Strengthening of Hippocampal Coupling Underlies MSN Recruitment to the Cocaine Zone

To distinguish whether strengthening of hippocampal coupling is uniform or location specific (Figure 4A), we fit a GLM to find connection weights that optimally predict MSN activity based solely on HPC activity (Figure 4B). We then used this model to generate predictions of each MSN spike train, from which we calculated a firing rate index (see STAR Methods). Although the model contains no explicit location information, the firing rate indices predicted from HPC activity were significantly correlated with the observed firing rate indices (n = 531, 713 MSNs; PRE $R = 0.45$, $p = 1.2 \times 10^{-7}$; POST $R = 0.59$, $p = 6.8 \times 10^{-68}$; Figure 4C).

We next examined the PYR to MSN connection weights and found that they increased in magnitude after cocaine conditioning (n = 4,047, 3,979 weights, rank sum test, $p = 1.2 \times 10^{-9}$; Figure 4D). In PRE sessions there was no difference between connection strengths from PYRs encoding the cocaine and saline zones (n = 2,011, 2,036 weights, rank sum test, $p = 0.10$; Figure 4E), but in POST sessions connection weights arising from cocaine zone PYRs were significantly larger (n = 2,014, 1,981 weights, rank sum test, $p = 1.4 \times 10^{-6}$; Figure 4F), consistent with connection weights being strengthened in a location-specific fashion. To test whether the location-specific distribution of connection weights was responsible for the recruitment of MSN activity in our model, we adjusted connection weights to equalize the distributions for PYRs encoding the cocaine and saline zones. In models fit to PRE sessions, this adjustment caused no change in MSN firing rate index (n = 531 MSNs, signed rank test, $p = 0.39$, Figure 4G). However, in models fit to POST sessions the MSN firing rate indices shifted away from the cocaine

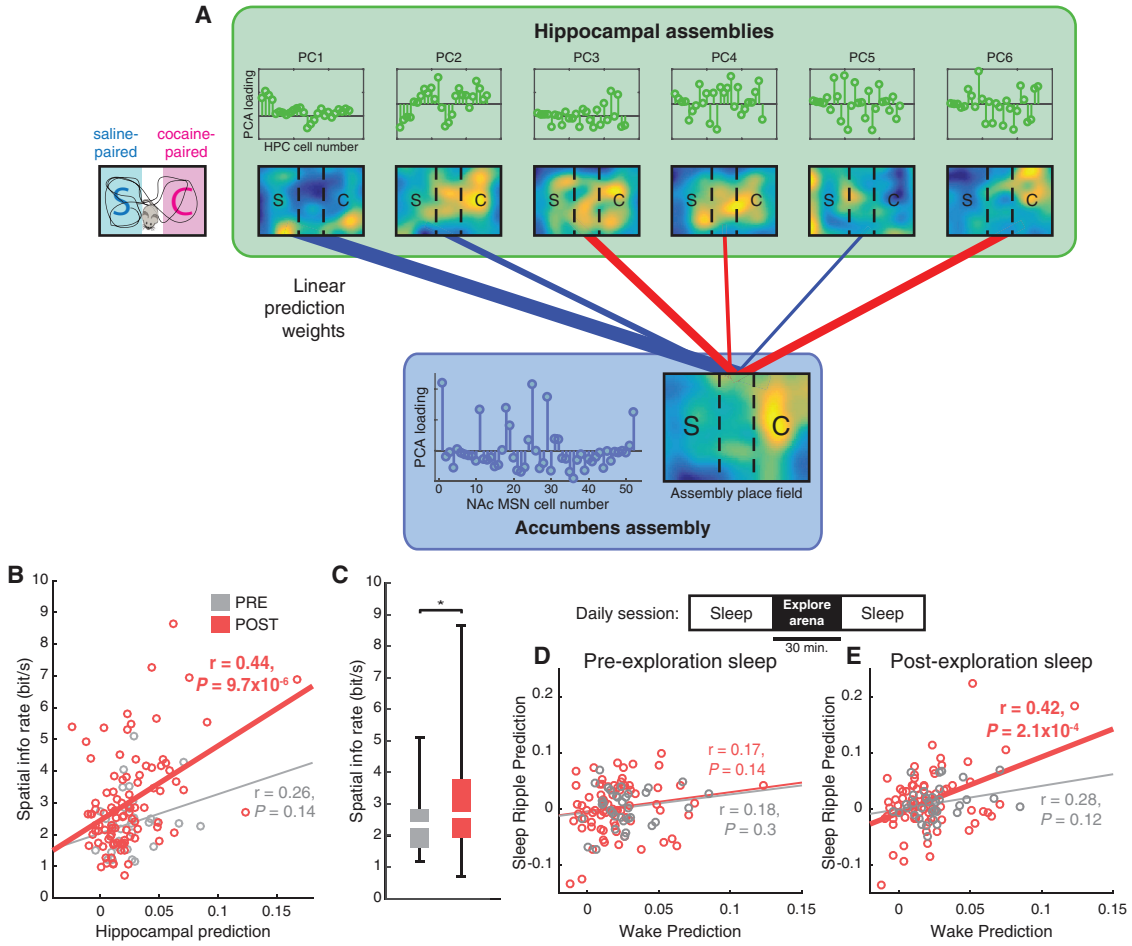

Figure 3. Cocaine Conditioning Increases the Strength of Functional Coupling between Hippocampal PYRs and Accumbens MSNs

(A) Activity of PYR assemblies predicts activity of MSN assemblies.

(B) The spatial information rate of an MSN assembly is correlated with the accuracy by which its activity can be predicted from PYR assemblies, in POST ($R = 0.44$, $p = 9.7 \times 10^{-6}$), but not PRE ($R = 0.26$, $p = 0.14$), sessions.

(C) Spatial information rate of MSN assemblies increases after cocaine conditioning (rank sum test, *$p = 0.02$).

(D) Model predictions for MSN assemblies during awake locomotion are uncorrelated with model predictions during sharp-wave ripples in pre-exploration sleep.

(E) Model predictions during awake locomotion are correlated with predictions during sharp-wave ripples in post-exploration sleep in POST ($p = 2.1 \times 10^{-4}$), but not PRE ($p = 0.12$), sessions. This suggests that cocaine conditioning strengthens coordinated hippocampus-accumbens replay.

zone ($n = 713$ MSNs, signed rank test, $p = 3.4 \times 10^{-8}$, Figure 4H), indicating that connection weight asymmetry contributes to MSN recruitment to the cocaine zone.

Since cocaine conditioning also increases PYR place field density in the cocaine zone (Figures S4A and S4B), we performed a similar analysis to determine the relative contribution of place field density to location-specific MSN activity. In PRE sessions there was no difference in distribution of PYR firing rate index magnitudes (Figure S4C), but in POST sessions the magnitude of the indices was larger for cocaine zone PYRs ($n = 164$, 205 PYRs, median 0.15 versus 0.24; rank sum test, $p = 2.6 \times 10^{-4}$, Figure S4D), confirming that place cells overrepresent the cocaine zone. Adjusting PYR spike trains to remove the asymmetry in PYR firing rate indices caused no change in MSN firing rate indices in PRE session models ($n = 531$ MSNs, signed rank test, $p = 0.83$, Figure S4E), but in POST session models the MSN firing rate indices shifted away from the cocaine zone ($n = 713$ MSNs, signed rank test, $p = 5.4 \times 10^{-4}$, Figure S4F), indicating that changes in PYR place field density contribute to MSN recruitment to the cocaine zone. Since place field changes and connection weight changes both contributed to increased MSN activity in the cocaine zone, we compared them directly to determine which was a larger contributor. The two effects contributed equally to the location tuning properties of MSNs encoding the saline zone ($n = 355$ MSNs, signed rank test, $p = 0.29$, Figure S4G), but for MSNs encoding the cocaine zone, changes in connection weights were a larger contributor than changes in PYR place fields ($n = 340$ MSNs, signed rank test, $p = 5.5 \times 10^{-9}$, Figure S4H).

To address the possibility that correlations between activity in HPC and NAc could be brought about by environmental cues, behavior, or common inputs, we analyzed the effect of

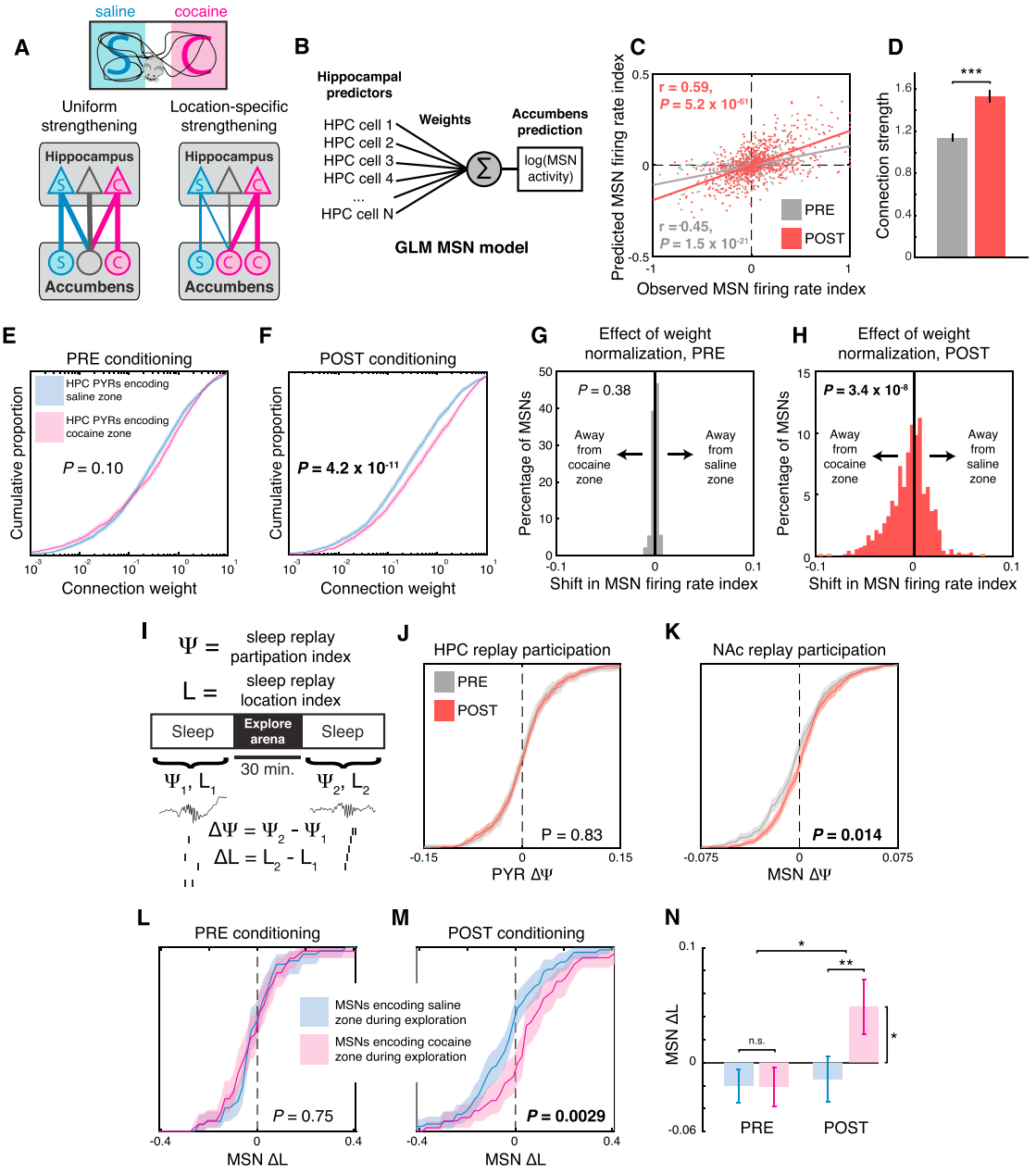

Figure 4. Cocaine Place Conditioning Preferentially Strengthens Coupling between MSNs and Hippocampal Pyramidal Cells Encoding the Cocaine-Paired Location

(A) Two models: cocaine could either uniformly strengthen all hippocampal inputs equally or preferentially strengthen the inputs that encode the cocaine-paired location.

(B) A GLM that predicts MSN spiking activity from PYR spiking activity by fitting connection weights can estimate the effects of modifying the connections.

(C) Model-predicted MSN firing rate indices based solely on hippocampal activity are significantly correlated with observed MSN firing rate indices ($R = 0.45$, $p = 1.2 \times 10^{-7}$ PRE; $R = 0.59$, $p = 6.8 \times 10^{-68}$ POST).

(D) Estimated connection weights are increased after cocaine conditioning (rank sum test, ***$p = 1.2 \times 10^{-9}$). Graph represents mean ± SEM.

(E) In PRE sessions, connection weights from cocaine zone-encoding PYRs and saline zone-encoding PYRs have equal distributions.

(F) In POST sessions, connections from cocaine zone-encoding PYRs have stronger weights than connections from saline zone-encoding PYRs (rank sum test, $p = 4.2 \times 10^{-11}$).

(G) In PRE sessions, adjusting connection weights from cocaine zone-encoding PYRs to match the distribution of weights from saline zone-encoding does not change predicted MSN firing rate indices.

(H) In POST sessions, normalizing connection weights from cocaine zone-encoding PYRs significantly shifts predicted MSN firing rate indices away from the cocaine zone (t test, $p = 3.4 \times 10^{-8}$), suggesting that the asymmetric connection weight distribution underlies increased MSN activity in the cocaine zone.

(legend continued on next page)

hippocampal replay events during sleep on MSN firing (Figure 4I, STAR Methods). By training a Bayesian decoder on HPC spike trains during awake exploration (Brown et al., 1998; Zhang et al., 1998), we were able to decode the locations encoded by replay events occurring during sleep. We found that HPC PYRs participated equally in replay events encoding the cocaine or saline zones (rank sum test, participation index 0.001 ± 0.003 PRE versus 0.004 ± 0.002 POST, n = 231, 341 PYRs, p = 0.83, Figure 4J), but in POST sessions NAc MSNs showed increased participation in replays encoding the cocaine zone (rank sum test, −0.002 ± 0.001 PRE versus 0.002 ± 0.001 POST, n = 344, 381 MSNs, p = 0.014, Figure 4K), consistent with a location-specific distribution of connection strengthening. To verify that the strengthened inputs we measured during sleep replays were related to the additional MSN firing in the cocaine zone, we calculated a location index L for each MSN, which represents the mean location encoded by replay events in which that MSN participated (see STAR Methods). We found that MSNs in POST sessions that encoded the cocaine zone during exploration had an elevated ΔL, indicating that they also fired preferentially during sleep replays encoding the cocaine zone (PRE ΔL −0.007 ± 0.015 saline, −0.013 ± 0.017 cocaine; POST ΔL −0.032 ± 0.020 saline, 0.056 ± 0.024 cocaine, n = 55, 52 PRE; n = 76, 54 POST, rank sum test, p = 0.0029, Figures 4L–4N). These results suggest that MSN firing in the cocaine zone depends on location-specific strengthening of HPC inputs to the NAc.

DISCUSSION

In this study, we found that cocaine place conditioning recruits mainly D2-positive NAc MSNs, and to a lesser extent hippocampal PYRs, to fire in the cocaine-paired zone. Additionally, MSNs receiving strong PYR inputs encoded more spatial information and were preferentially recruited to the cocaine zone, suggesting that PYR inputs were driving MSN cocaine zone activity. Finally, we found that cocaine conditioning strengthens coupling between HPC PYRs and NAc MSNs in a location-dependent fashion during both waking and sleep.

Although extracellular recording is not able to make direct measurements of synaptic strength, *ex vivo* slice experiments have shown that repeated cocaine exposure potentiates hippocampal inputs to NAc MSNs (Britt et al., 2012; MacAskill et al., 2014; Pascoli et al., 2014), and our findings are consistent with this plasticity underlying the location-specific increase in hippocampus-NAc coupling. The majority of our POST sessions were recorded in early abstinence (<2 weeks), and our finding of recruitment of D2+ MSNs to fire in the cocaine zone is consistent with the results of MacAskill et al. (MacAskill et al., 2014), who found that cocaine conditioning increased the D2/D1 ratio of HPC inputs to the NAc. On the other hand, Pascoli et al. (Pascoli et al., 2014) found selective potentiation of HPC inputs onto D1-positive MSNs, but only in late cocaine abstinence (>2 weeks). A limitation of our study is that we primarily examined early abstinence, and understanding the longer-term effects of cocaine conditioning will be the focus of future work. Our results also suggest that cocaine may preferentially strengthen the inputs that are most active at the time of cocaine exposure, which could differ depending on the subregion of accumbens and environmental factors during conditioning.

It is worth emphasizing that our place conditioning paradigm (Figure S2A) pairs cocaine with a spatial location defined relative to distal navigational cues, and proximal sensory cues were minimized and counterbalanced across cocaine/saline conditions. Under similar conditions, CPP has been shown to be dependent on dorsal hippocampus and not ventral hippocampus or amygdala (Ferbinteanu and McDonald, 2001; Meyers et al., 2003; Trouche et al., 2016). In CPP paradigms incorporating proximal sensory cues that differ between the cocaine and saline zones, NAc inputs from other structures such as the amygdala would likely be affected as well.

Our results may appear different from those of German et al. (German and Fields, 2007), who recorded neurons in the NAc during CPP POST sessions in rats and found that NAc MSNs exhibit decreased firing rates in the drug-paired zone. The most likely explanation for this difference is the fact that their study used morphine, and ours used cocaine. Cocaine and morphine act through different molecular mechanisms and are known to induce opposite changes in NAc dendritic spine density (Robinson and Kolb, 1999a, 1999b). Our results suggest that they may induce CPP through different physiological mechanisms at the level of the NAc as well. A recent study by Calipari et al. (Calipari et al., 2016) using fiber photometry appears to contradict our findings directly, as they used cocaine CPP and reported increased population activity in D1 cells and decreased activity in D2 cells in the cocaine zone in early abstinence. There are several possible explanations for this discrepancy, including

(I) Sleep replay analysis. During post-exploration sleep, the hippocampus replays spatial trajectories from inside the arena, but replay during pre-exploration sleep encodes locations outside the arena. The participation index Ψ represents the relative likelihood of a cell firing during replays encoding the cocaine zone versus saline zone. A location index L is also calculated for each MSN, representing the average spatial location encoded by replay events that drove that MSN to fire, with −1 representing the saline zone and +1 representing the cocaine zone. $\Delta\Psi$ and ΔL are the differences in Ψ and L, respectively, between post- and pre-exploration sleep.

(J) HPC PYR participation index Ψ does not change from PRE to POST, indicating that the PYR firing rate is the same in ripples encoding either location.

(K) For NAc MSNs, the Ψ index increases from PRE to POST (rank sum test, p = 0.014), indicating that in POST sessions, MSNs fire more spikes during sleep replays encoding the cocaine zone.

(L) In PRE sessions, MSNs that fired preferentially in either the cocaine or saline zones during exploration showed no difference in ΔL.

(M) In POST sessions, cocaine zone MSNs exhibited a larger ΔL than saline zone MSNs (rank sum test, **p = 0.0029), indicating that the MSNs that fire preferentially during sleep replay events encoding the cocaine zone are the same MSNs that fire preferentially during awake exploration of the cocaine zone. All shaded areas represent 99% confidence intervals.

(N) This effect is significantly different between PRE and POST sessions (two-way ANOVA, *p = 0.0197), and only the cocaine zone MSNs in POST sessions showed a ΔL that was significantly different from zero (signed rank test, *p = 0.014). Graph represents mean ± SEM.

differences in the conditioning protocol, nonlinear relationships between spike rate and calcium signal, inability to distinguish MSN and interneuron calcium signals, and the fact that we used GLMs to regress out movement-related MSN activity.

Location-dependent plasticity supports a plausible mechanistic model of cocaine CPP in which the NAc acts as an action-location-outcome associator (Berke and Hyman, 2000; van der Meer and Redish, 2011b). We hypothesize that the NAc integrates hippocampal inputs encoding a spatial location and prefrontal cortical inputs encoding an action plan to generate actions appropriate for a given spatial context. Under physiological conditions, performing an action in a specific location that generates a positive reward prediction error causes dopamine release in the NAc (Hart et al., 2014). This would strengthen hippocampal synapses encoding the rewarded location (Reynolds and Wickens, 2002), increasing the expected reward outcome associated with that action/location pairing. During cocaine place conditioning, NAc dopamine levels are artificially elevated, effectively rewarding all actions performed in the cocaine zone and increasing the strength of hippocampal inputs encoding that location. Upon exposure to the cocaine zone in POST sessions, the strengthened hippocampal inputs would drive increased firing in NAc MSNs, leading the animal to engage in activity in the cocaine zone rather than run to the saline zone. Determining whether this model is correct will require further studies involving multisite unit recording and manipulation of prefrontal cortex in CPP.

It is believed that drugs of abuse exert differential effects at various synaptic pathways in the brain—our results suggest that synaptic changes may be specific even at the level of functionally defined subsets of synapses within a single synaptic pathway. One important consequence of non-uniform changes in synaptic strength is that behavior could be driven by changes in a subset of synapses in a projection, while the average strength of the entire projection could be unchanged or even change in the opposite direction. This reveals an additional layer of complexity that is not recognized in many circuit models of drug addiction and suggests that some of these models may require revision. Selective plasticity of specific corticostriatal synapses based on presynaptic firing properties has been observed in other striatal regions (Xiong et al., 2015) and may represent a canonical mechanism by which sensory and contextual information can bias action selection based on reward history.

STAR★METHODS

Detailed methods are provided in the online version of this paper and include the following:

- KEY RESOURCES TABLE
- CONTACT FOR REAGENT AND RESOURCE SHARING
- EXPERIMENTAL MODEL AND SUBJECT DETAILS
  - Animal models
  - Viral vectors
- METHOD DETAILS
  - Stereotactic surgery and data acquisition
  - Recording sessions and behavioral conditioning
- QUANTIFICATION AND STATISTICAL ANALYSIS
  - Firing rate and behavior indices
  - Generalized linear models (GLMs)
  - Information measures
  - Principal component analysis (PCA)
  - Assembly prediction analysis
  - Connection weight modeling
  - Place field shifting and connection weight scaling
  - Sleep replay analysis
  - Statistical analysis
- DATA AND SOFTWARE AVAILABILITY

SUPPLEMENTAL INFORMATION

Supplemental Information includes four figures and two tables and can be found with this article online at https://doi.org/10.1016/j.neuron.2018.04.015.

ACKNOWLEDGMENTS

The authors thank Gord Fishell, Lisa Roux, Viola Woo, Sujit Thomas, and the members of the Buzsáki lab for support, technical assistance, and comments on the manuscript. This work was supported by the Leon Levy Foundation (L.S.), the Brain and Behavior Research Foundation (L.S.), and NIH grants K08 DA036657 (L.S.) and MH107396 (G.B.).

AUTHOR CONTRIBUTIONS

Conceptualization, L.S. and G.B. Investigation, L.S., A.C., and D.C. Formal Analysis, L.S., A.P., and A.C. Writing, L.S. and G.B.

DECLARATION OF INTERESTS

The authors have no conflicts of interest to report.

Received: February 28, 2017
Revised: November 21, 2017
Accepted: April 13, 2018
Published: May 10, 2018

REFERENCES

Barthó, P., Hirase, H., Monconduit, L., Zugaro, M., Harris, K.D., and Buzsáki, G. (2004). Characterization of neocortical principal cells and interneurons by network interactions and extracellular features. J. Neurophysiol. *92*, 600–608.

Berenyi, A., Somogyvari, Z., Nagy, A.J., Roux, L., Long, J.D., Fujisawa, S., Stark, E., Leonardo, A., Harris, T.D., and Buzsaki, G. (2014). Large-scale, high-density (up to 512 channels) recording of local circuits in behaving animals. J. Neurophysiol. *111*, 1132–1149.

Berke, J.D., and Hyman, S.E. (2000). Addiction, dopamine, and the molecular mechanisms of memory. Neuron *25*, 515–532.

Britt, J.P., Benaliouad, F., McDevitt, R.A., Stuber, G.D., Wise, R.A., and Bonci, A. (2012). Synaptic and behavioral profile of multiple glutamatergic inputs to the nucleus accumbens. Neuron *76*, 790–803.

Brown, E.N., Frank, L.M., Tang, D., Quirk, M.C., and Wilson, M.A. (1998). A statistical paradigm for neural spike train decoding applied to position prediction from ensemble firing patterns of rat hippocampal place cells. J. Neurosci. *18*, 7411–7425.

Buzsáki, G., Leung, L.W., and Vanderwolf, C.H. (1983). Cellular bases of hippocampal EEG in the behaving rat. Brain Res. *287*, 139–171.

Buzsáki, G., Horvath, Z., Urioste, R., Hetke, J., and Wise, K. (1992). High-frequency network oscillation in the hippocampus. Science *256*, 1025–1027.

Calabresi, P., Centonze, D., Gubellini, P., Marfia, G.A., and Bernardi, G. (1999). Glutamate-triggered events inducing corticostriatal long-term depression. J. Neurosci. *19*, 6102–6110.

Calipari, E.S., Bagot, R.C., Purushothaman, I., Davidson, T.J., Yorgason, J.T., Peña, C.J., Walker, D.M., Pirpinias, S.T., Guise, K.G., Ramakrishnan, C., et al. (2016). In vivo imaging identifies temporal signature of D1 and D2 medium spiny neurons in cocaine reward. Proc. Natl. Acad. Sci. USA *113*, 2726–2731.

Ferbinteanu, J., and McDonald, R.J. (2001). Dorsal/ventral hippocampus, fornix, and conditioned place preference. Hippocampus *11*, 187–200.

German, P.W., and Fields, H.L. (2007). Rat nucleus accumbens neurons persistently encode locations associated with morphine reward. J. Neurophysiol. *97*, 2094–2106.

Harris, K.D., Henze, D.A., Csicsvari, J., Hirase, H., and Buzsáki, G. (2000). Accuracy of tetrode spike separation as determined by simultaneous intracellular and extracellular measurements. J. Neurophysiol. *84*, 401–414.

Harris, K.D., Csicsvari, J., Hirase, H., Dragoi, G., and Buzsáki, G. (2003). Organization of cell assemblies in the hippocampus. Nature *424*, 552–556.

Hart, A.S., Rutledge, R.B., Glimcher, P.W., and Phillips, P.E. (2014). Phasic dopamine release in the rat nucleus accumbens symmetrically encodes a reward prediction error term. J. Neurosci. *34*, 698–704.

Ito, R., Robbins, T.W., Pennartz, C.M., and Everitt, B.J. (2008). Functional interaction between the hippocampus and nucleus accumbens shell is necessary for the acquisition of appetitive spatial context conditioning. J. Neurosci. *28*, 6950–6959.

Jones, M.W., and Wilson, M.A. (2005). Theta rhythms coordinate hippocampal-prefrontal interactions in a spatial memory task. PLoS Biol. *3*, e402.

Kim, S.M., Ganguli, S., and Frank, L.M. (2012). Spatial information outflow from the hippocampal circuit: distributed spatial coding and phase precession in the subiculum. J. Neurosci. *32*, 11539–11558.

Komorowski, R.W., Garcia, C.G., Wilson, A., Hattori, S., Howard, M.W., and Eichenbaum, H. (2013). Ventral hippocampal neurons are shaped by experience to represent behaviorally relevant contexts. J. Neurosci. *33*, 8079–8087.

Lansink, C.S., Goltstein, P.M., Lankelma, J.V., Joosten, R.N., McNaughton, B.L., and Pennartz, C.M. (2008). Preferential reactivation of motivationally relevant information in the ventral striatum. J. Neurosci. *28*, 6372–6382.

Lansink, C.S., Goltstein, P.M., Lankelma, J.V., McNaughton, B.L., and Pennartz, C.M. (2009). Hippocampus leads ventral striatum in replay of place-reward information. PLoS Biol. *7*, e1000173.

Lavoie, A.M., and Mizumori, S.J. (1994). Spatial, movement- and reward-sensitive discharge by medial ventral striatum neurons of rats. Brain Res. *638*, 157–168.

Lee, A.K., and Wilson, M.A. (2002). Memory of sequential experience in the hippocampus during slow wave sleep. Neuron *36*, 1183–1194.

MacAskill, A.F., Cassel, J.M., and Carter, A.G. (2014). Cocaine exposure reorganizes cell type- and input-specific connectivity in the nucleus accumbens. Nat. Neurosci. *17*, 1198–1207.

McCormick, D.A., Connors, B.W., Lighthall, J.W., and Prince, D.A. (1985). Comparative electrophysiology of pyramidal and sparsely spiny stellate neurons of the neocortex. J. Neurophysiol. *54*, 782–806.

Meyers, R.A., Zavala, A.R., and Neisewander, J.L. (2003). Dorsal, but not ventral, hippocampal lesions disrupt cocaine place conditioning. Neuroreport *14*, 2127–2131.

Miyazaki, K., Mogi, E., Araki, N., and Matsumoto, G. (1998). Reward-quality dependent anticipation in rat nucleus accumbens. Neuroreport *9*, 3943–3948.

Nádasdy, Z., Hirase, H., Czurkó, A., Csicsvari, J., and Buzsáki, G. (1999). Replay and time compression of recurring spike sequences in the hippocampus. J. Neurosci. *19*, 9497–9507.

O'Keefe, J. (1976). Place units in the hippocampus of the freely moving rat. Exp. Neurol. *51*, 78–109.

Pascoli, V., Terrier, J., Espallergues, J., Valjent, E., O'Connor, E.C., and Lüscher, C. (2014). Contrasting forms of cocaine-evoked plasticity control components of relapse. Nature *509*, 459–464.

Peyrache, A., Khamassi, M., Benchenane, K., Wiener, S.I., and Battaglia, F.P. (2009). Replay of rule-learning related neural patterns in the prefrontal cortex during sleep. Nat. Neurosci. *12*, 919–926.

Peyrache, A., Benchenane, K., Khamassi, M., Wiener, S.I., and Battaglia, F.P. (2010). Principal component analysis of ensemble recordings reveals cell assemblies at high temporal resolution. J. Comput. Neurosci. *29*, 309–325.

Peyrache, A., Lacroix, M.M., Petersen, P.C., and Buzsáki, G. (2015). Internally organized mechanisms of the head direction sense. Nat. Neurosci. *18*, 569–575.

Phillipson, O.T., and Griffiths, A.C. (1985). The topographic order of inputs to nucleus accumbens in the rat. Neuroscience *16*, 275–296.

Reynolds, J.N., and Wickens, J.R. (2002). Dopamine-dependent plasticity of corticostriatal synapses. Neural Netw. *15*, 507–521.

Robinson, T.E., and Kolb, B. (1999a). Alterations in the morphology of dendrites and dendritic spines in the nucleus accumbens and prefrontal cortex following repeated treatment with amphetamine or cocaine. Eur. J. Neurosci. *11*, 1598–1604.

Robinson, T.E., and Kolb, B. (1999b). Morphine alters the structure of neurons in the nucleus accumbens and neocortex of rats. Synapse *33*, 160–162.

Schmitzer-Torbert, N.C., and Redish, A.D. (2008). Task-dependent encoding of space and events by striatal neurons is dependent on neural subtype. Neuroscience *153*, 349–360.

Skaggs, W.E., and McNaughton, B.L. (1996). Replay of neuronal firing sequences in rat hippocampus during sleep following spatial experience. Science *271*, 1870–1873.

Skaggs, W.E., McNaughton, B.L., Gothard, K.M., and Markus, E.J. (1993). An information-theoretic approach to deciphering the hippocampal code. In Advances in Neural Information Processing Systems 5, S.J. Hanson, C.L. Giles, and J.D. Cowan, eds. (Morgan Kaufmann), pp. 1030–1037.

Stark, E., Koos, T., and Buzsáki, G. (2012). Diode probes for spatiotemporal optical control of multiple neurons in freely moving animals. J. Neurophysiol. *108*, 349–363.

Tabuchi, E.T., Mulder, A.B., and Wiener, S.I. (2000). Position and behavioral modulation of synchronization of hippocampal and accumbens neuronal discharges in freely moving rats. Hippocampus *10*, 717–728.

Trouche, S., Perestenko, P.V., van de Ven, G.M., Bratley, C.T., McNamara, C.G., Campo-Urriza, N., Black, S.L., Reijmers, L.G., and Dupret, D. (2016). Recoding a cocaine-place memory engram to a neutral engram in the hippocampus. Nat. Neurosci. *19*, 564–567.

Truccolo, W., Eden, U.T., Fellows, M.R., Donoghue, J.P., and Brown, E.N. (2005). A point process framework for relating neural spiking activity to spiking history, neural ensemble, and extrinsic covariate effects. J. Neurophysiol. *93*, 1074–1089.

van der Meer, M.A., and Redish, A.D. (2011a). Theta phase precession in rat ventral striatum links place and reward information. J. Neurosci. *31*, 2843–2854.

van der Meer, M.A., and Redish, A.D. (2011b). Ventral striatum: a critical look at models of learning and evaluation. Curr. Opin. Neurobiol. *21*, 387–392.

van der Meer, M.A., Johnson, A., Schmitzer-Torbert, N.C., and Redish, A.D. (2010). Triple dissociation of information processing in dorsal striatum, ventral striatum, and hippocampus on a learned spatial decision task. Neuron *67*, 25–32.

Xiong, Q., Znamenskiy, P., and Zador, A.M. (2015). Selective corticostriatal plasticity during acquisition of an auditory discrimination task. Nature *521*, 348–351.

Yamin, H.G., Stern, E.A., and Cohen, D. (2013). Parallel processing of environmental recognition and locomotion in the mouse striatum. J. Neurosci. *33*, 473–484.

Zhang, K., Ginzburg, I., McNaughton, B.L., and Sejnowski, T.J. (1998). Interpreting neuronal population activity by reconstruction: unified framework with application to hippocampal place cells. J. Neurophysiol. *79*, 1017–1044.

STAR★METHODS

KEY RESOURCES TABLE

REAGENT or RESOURCE	SOURCE	IDENTIFIER
Bacterial and Virus Strains		
AAV-EF1a-DIO-hChR2(H134R)-EYFP	University of North Carolina	N/A
Experimental Models: Organisms/Strains		
Mice: C57BL/6J (male)	Jackson	RRID: IMSR_JAX:000664
Mice: FVB/NJ (female)	Jackson	RRID: IMSR_JAX:001800
Mice: Drd1a-Cre: B6.FVB(Cg)-Tg(Drd1a-cre)EY217Gsat/Mmucd	MMRRC	RRID: MMRRC_034258-UCD
Mice: A2a-Cre: B6.FVB(Cg)-Tg(Adora2a-cre)KG139Gsat/Mmucd	MMRRC	RRID: MMRRC_036158-UCD
Mice: Ai32: B6.Cg-Gt(ROSA)26Sor$^{tm32(CAG-COP4*H134R/EYFP)Hze}$/J	Jackson	RRID: IMSR_JAX:024109
Software and Algorithms		
MATLAB	MATLAB	https://www.mathworks.com/
Custom-written MATLAB code for data analysis	This lab	Request from Lead Contact
Neurosuite	Lynn Hazan, Michael Zugaro	http://neurosuite.sourceforge.net/
Other		
Amplipex 256 channel recording system	Amplipex Ltd	http://www.amplipex.com/
Silicon probes	Neuronexus	Buzsaki64sp and Buzsaki5x12
LightHUB laser, 473 nm wavelength	Omicron Laser	LightHUB-2

CONTACT FOR REAGENT AND RESOURCE SHARING

Further information and requests for resources and reagents should be directed to and will be fulfilled by the Lead Contact, György Buzsáki (gyorgy.buzsaki@nyumc.org).

EXPERIMENTAL MODEL AND SUBJECT DETAILS

Animal models

Procedures were conducted using two BAC transgenic lines from GENSAT: Drd1a-Cre, (B6.FVB(Cg)-Tg(Drd1a-cre)EY217Gsat/Mmucd; RRID: MMRRC_034258-UCD) and A2a-Cre, (B6.FVB(Cg)-Tg(Adora2a-cre)KG139Gsat/Mmucd; RRID: MMRRC_036158UCD) and one knockin line from the Allen Institute: Ai32 Cre-dependent channelrhodopsin line (B6.Cg-Gt(ROSA)26Sor$^{tm32(CAG-COP4*H134R/EYFP)Hze}$/J; RRID: IMSR_JAX:024109). Experiments described in this study were conducted using 16 male mice in total (25-40 g, 12-30 weeks of age). 6 mice were wild-type C57BL/6J x FVB hybrids, 7 mice were Drd1a-Cre; Ai32 mice on a C57BL/6J background, and 3 mice were A2a-Cre; Ai32 mice on a C57BL/6J background. After implantation, animals were housed individually on a 12/12 h day/night schedule and were given *ad libitum* access to food and water. All experiments were conducted in accordance with the Institutional Animal Care and Use Committee of New York University Medical Center.

Viral vectors

Adeno-associated viral vector (AAV) was used to express channelrhodopsin-2 in Cre-expressing neurons in the ventral striatum of D1-cre mice. The recombinant AAV vector was pseudotyped with AAV5 capsid protein and packaged by the University of North Carolina viral core.

METHOD DETAILS

Stereotactic surgery and data acquisition

All animals were implanted with either 32- or 64-site silicon probes (NeuroNexus) in posterior CA1 (AP −3.2 mm, ML 3 mm, DV ~1.5 mm) and in nucleus accumbens (AP 1.5 mm, ML 1.4 mm, DV 3.8 mm from brain surface) under isoflurane anesthesia, as described previously (Stark et al., 2012). Ground and reference wires were implanted in the skull above the cerebellum, and a grounded copper mesh hat was constructed shielding the probes. Probes were mounted on microdrives that were advanced to the CA1 pyramidal layer over the course of 3-5 days after surgery, and CA1 was identified by the presence of sharp wave ripple oscillations (Buzsáki et al., 1992). Animals were allowed to recover for at least one week prior to behavioral testing. After implantation,

all animals were housed individually. Recordings were performed at 20 kHz using a 256-channel Amplipex system (Berenyi et al., 2014), and the animal's position was determined by tracking the position of red and blue LEDs mounted on the recording headstage. Offline spike sorting was performed using KlustaKwik (Harris et al., 2000), followed by manual adjustment using Klusters. Isolated single units were assigned a putative cell type based on established criteria in the hippocampus (Barthó et al., 2004; McCormick et al., 1985) (Figure S1B) and striatum (Schmitzer-Torbert and Redish, 2008; Yamin et al., 2013) (Figure S1C). Recording location was confirmed by electrolytic lesioning and histology (Figures S1F and S1G). Optotagging analysis was performed in D1-cre mice injected with AAV-FLEX-ChR2-EYFP or in Adora2A-cre; Ai32 mice that expressed ChR2 from a genomic locus. Units were defined as optically tagged based on published criteria (Stark et al., 2012), using a p value cutoff of 10^{-4} and a modulation index cutoff of 0.6 (Figure S1D). Putative D1 and D2 MSNs met the dual criteria of optogenetic response and classification as MSN based on waveform and bursting criteria. We found that >50% of tagged units responded in 5 ms or less (Figure S1E), and restricting our analysis to the subset of neurons with <5 ms did not qualitatively change the results.

Recording sessions and behavioral conditioning

Animals were housed on a 12-hour light/dark cycle, and all recording sessions occurred 1-2 hr prior to the onset of the dark phase. For all recording sessions, animals were recorded while in the home cage for 30-60 min both prior to and after exploration of the CPP arena. During the first 1-3 days, animals were recorded in PRE sessions, in which they explored the CPP arena for 30 min (Figure S2A). During five subsequent daily conditioning sessions, animals were injected with IP saline and confined to one side of the arena for 30 min, then returned to the home cage for 5 min. During this time, the CPP arena was cleaned and rotated 180°, and the animal was then injected with cocaine (15 mg/kg IP) and placed in the cocaine zone for 30 min. The cocaine zone was defined as the side of the arena the animal intrinsically preferred *less* during PRE sessions. The CPP arena was a featureless, symmetrical Plexiglas box designed to minimize local sensory cues. However, the side within the CPP arena in which the animal was conditioned changed daily, but the animal's absolute room location ('place') during saline and cocaine pairing was constant from one day to the next. After five daily conditioning sessions, the animals were recorded in daily POST conditioning sessions in which conditions were identical to the PRE sessions. The strength of behavioral place preference tended to decrease with each POST session, and analysis of POST sessions was restricted to sessions in which the animal showed a place preference for the cocaine zone.

QUANTIFICATION AND STATISTICAL ANALYSIS

Firing rate and behavior indices

To quantify the relative firing rate of a cell in the saline and cocaine zones, we created a firing rate index φ defined as

$$\varphi \equiv \frac{C - S}{C + S}$$

where C is the firing rate of the cell in the cocaine zone, and S is the firing rate of the cell in the saline zone. A cell with $\varphi = 0$ has an equal firing rate in both zones, while a cell with $\varphi = -1$ fires only in the saline zone, and a cell with $\varphi = 1$ fires only in the cocaine zone. For analysis of behavior (Figures 1G–1I), we created a behavior index η defined as

$$\eta \equiv \frac{t_C - t_S}{t_C + t_S}$$

where t_C is the amount of time the animal spends in the cocaine zone, and t_S is the amount of time the animal spends in the saline zone. Analogously, in a recording session with $\eta = 0$, the animal spends an equal amount of time in both zones. If $\eta = -1$, the animal spends the entire session in the saline zone, and if $\eta = 1$, the animal spends the entire session in the cocaine zone.

Generalized linear models (GLMs)

Because running speed and spatial location are correlated in CPP (Figures S2B–S2E), we used GLMs to separate out the effects of these two variables. We tested several GLMs using 10-fold cross-validation (Harris et al., 2003; Peyrache et al., 2015; Truccolo et al., 2005). In this procedure, data are split into ten segments, and the GLM is trained on nine segments and tested on the last segment. This is repeated ten times so that each segment is tested once. The purpose of this procedure is to penalize model overfitting and allow direct comparison of GLMs containing different numbers of predictors. We found that the best predictions (Table S2) were with a GLM of the form

$$ln(Q_{MSN}(t)) = \beta_0 + \beta_1 X(t) + \beta_2 Z(t) + \varepsilon$$

where *X(t)* is a *location* indicator vector that is 1 when the animal is in the cocaine zone and 0 in the saline zone, *Z(t)* is the linear speed of the animal in cm/s, and ε is the residual. This produces a measurement of speed modulation that is independent of position (β_2) and enables us to calculate the corrected cocaine index φ_{corr} with running speed regressed out:

$$C_{corr} = \frac{e^{\beta_0} e^{\beta_1}}{binsize} \text{ and } S_{corr} = \frac{e^{\beta_0}}{binsize}$$

$$\varphi_{corr} = \frac{C_{corr} - S_{corr}}{C_{corr} + S_{corr}} = \frac{e^{\beta_1} - 1}{e^{\beta_1} + 1}$$

To include hippocampal activity as a predictor of MSN spike trains (Figure 3), we extended the GLM to include the first n significant PC scores $scPC_x$ (see PCA section below):

$$ln(Q_{MSN}(t)) = \beta_0 + \beta_1 X(t) + \beta_2 Z(t) + \beta_3 scPC_1(t) + \cdots + \beta_{n+2} scPC_n(t) + \varepsilon$$

Information measures

To compare the accuracy of different GLMs in predicting MSN spike trains, we used log-likelihood measures. Each GLM produces a predicted intensity function f, and the log-likelihood L_f of that intensity function producing the observed spike train (Stark et al.) is given by

$$L_f = \sum_s log_2(f(T_s)) - \int f(t)dt$$

which is in units of bits. The difference in GLM prediction quality is measured using the difference between the log-likelihoods R_x. When comparing GLMs with different numbers of predictors, this quantity represents the information about the predicted spike train carried by extra predictors in one GLM. We calculated the following R's:

$$R_{PYR} = L_{PYR} - L_0$$

$$R_{PYR-loc} = L_{PYR,loc} - L_{loc}$$

$$R_{PYR-spd} = L_{PYR,spd} - L_{spd}$$

R_{PYR} is the difference in L between a GLM containing hippocampal PYRs as predictors and a GLM containing no predictors (i.e., a constant baseline firing rate), and it represents the total information about MSN spiking carried by simultaneously recorded hippocampal pyramidal cells. $R_{PYR\text{-}loc}$ is the difference in L between a GLM containing PYRs and location and a GLM containing only location. $R_{PYR\text{-}loc}$ represents the additional information that PYRs carry about MSN spiking that is not location-related. The quantity $R_{PYR} - R_{PYR\text{-}loc}$ therefore represents the location-related information that PYRs carry about MSN spiking, and $R_{PYR} - R_{PYR\text{-}spd}$ represents the analogous information measure for running speed.

Principal component analysis (PCA)

PCA was applied on binned spike trains (25 ms bins). The number of significant principal components (PCs) was determined by the upper limit λ_{max} of the Marchenko-Pastur distribution (Peyrache et al., 2010; Peyrache et al., 2009)

$$\lambda_{max} = \left(1 + \sqrt{\frac{N}{B}}\right)^2$$

where B is the number of time bins and N the number of neurons. Binned spike trains were projected onto the significant PCs, resulting in a time series of activation of each individual PC, referred to as PC scores $scPC_x$.

Assembly prediction analysis

We first performed PCA separately on binned MSN and PYR spike trains to obtain correlated MSN and PYR assemblies, retaining only significant PCs. To quantify the functional relationship between these assemblies, we used a cross-validated procedure. During each training epoch, a single PC score of MSN data was linearly regressed against all significant PYR PC scores. The linear model was then used to construct a prediction of the MSN PC score during the test epoch. The likelihood of the prediction was measured by the correlation coefficient between the predicted and observed PC scores.

The same method was used to quantify the prediction during sleep sharp wave ripples. Each significant MSN PC score was linearly regressed against all hippocampal PC scores. The resulting linear model was used to build predictors of individual MSN PC scores during hippocampal ripples. The likelihood of the prediction was defined as the correlation coefficient between the prediction and the observed PC score during sharp wave ripples.

Connection weight modeling

To model spiking activity of MSNs using hippocampal PYR activity as predictors, we performed singular value decomposition (SVD) on the binned PYR spike trains. SVD was used instead of PCA because PCA effectively normalizes each PYR spike train, discarding

differences in firing rate of PYRs that could vary systematically with place field location. All connection weight analyses (Figure 4) were also performed with PCA and produced qualitatively similar results (not shown). SVD factorizes Q_{PYR}, which is the B x N_{PYR} matrix of binned PYR spike trains (B time bins, N_{PYR} PYRs):

$$Q_{PYR} = U \cdot S \cdot V^T$$

U and V are orthonormal matrices, and S is a diagonal matrix of eigenvalues that denote how much variance is accounted for by each column of U and V. Since the null distribution of eigenvalues can not be calculated analytically as in PCA, we performed parallel analysis to determine the number n of how many significant columns of U and V to retain. We then predicted a single binned MSN spike train $Q_{MSN}(t)$ using a GLM of the form:

$$\ln(Q_{MSN}(t)) = \beta_0 + \beta_1 U_1(t) S_{1,1} + \cdots + \beta_n U_n(t) S_{n,n} + \varepsilon = \beta_0 + \sum_{i=1}^{n} \beta_i U_i(t) S_{i,i} + \varepsilon$$

In matrix form, this becomes

$$\ln(Q_{MSN}) = \beta_0 + \tilde{U} \cdot \tilde{S} \cdot \vec{\beta} + \varepsilon$$

where $\tilde{U}$, $\tilde{S}$, and $\tilde{V}$ denote U, S, and V with only the first n columns retained, and $\vec{\beta}$ is the n x 1 vector of GLM coefficients. Because V is orthonormal, $V^{-1} = V^T$, therefore

$$Q_{PYR} \cdot \tilde{V} \cong \tilde{U} \cdot \tilde{S}$$

we substitute $Q_{PYR} \cdot \tilde{V}$ for $\tilde{U} \cdot \tilde{S}$ in the GLM equation yielding

$$\ln(Q_{MSN}) \cong \beta_0 + Q_{PYR} \cdot \left(\tilde{V} \cdot \vec{\beta} \right) + \varepsilon$$

Here, $(\tilde{V} \cdot \vec{\beta})$ is an N_{PYR} x 1 vector containing estimates of the connection weights between all N_{PYR} of the PYRs and a single MSN.

Place field shifting and connection weight scaling

We found that the distribution of PYR place field locations and connection weights was asymmetrical with respect to the cocaine/saline zones, meaning that the cocaine zone had a higher place field density and stronger connection weights (Figure 4, Figure S4). To determine the effects of this asymmetry, we adjusted the distribution of place field locations and connection weights in our model so that the distribution for PYRs encoding the cocaine zone matched PYRs encoding the saline zone. We then examined the changes in MSN spatial tuning predicted by the model to determine how much the asymmetries contributed to the additional MSN activity in the cocaine zone. To accomplish this, we first calculated the cumulative distribution functions (CDFs) of PYR cocaine index and connection weights for PYRs that encode the saline and cocaine zones (*i.e,.* with negative or positive cocaine indices). For the cocaine zone PYRs, we assigned each cocaine index or connection weight a percentile score within the cocaine zone PYRs, then adjusted each value to match the value from a corresponding saline zone PYR at the same percentile within saline zone PYRs. This had the effect of making the CDFs of PYR cocaine index or connection weight identical for PYRs encoding the saline and cocaine zones.

To adjust PYR place field location, we calculated location-dependent scaling factors so that each spike would contribute a non-integer value slightly more or less than 1.0 to the binned spike train, depending on which zone the animal was in when the spike occurred. To obtain unique solutions, we also enforced a constraint that the sum of the binned spike train (i.e., the "firing rate") over the entire trial would be unchanged. We started with the adjusted cocaine index

$$\varphi_{adj} = \frac{C_{adj} - S_{adj}}{C_{adj} + S_{adj}}$$

with the firing rate constraint: $Ct_C + St_S = C_{adj} t_C + S_{adj} t_S$

where C and S are PYR firing rates in the cocaine and saline zones, and t_C and t_S are the amount of time spent in the cocaine and saline zones, respectively. We then determined the location-dependent scaling factors to multiply with each element of the binned spike train to adjust the cocaine index to equal φ_{adj}

$$\frac{S_{adj}}{S} = \frac{(\varphi_{adj} - 1)(Ct_C + St_S)}{St_S(\varphi_{adj} - 1) - St_C(\varphi_{adj} + 1)}$$

$$\frac{C_{adj}}{C} = \frac{(\varphi_{adj} + 1)(Ct_C + St_S)}{Ct_C(\varphi_{adj} + 1) - Ct_S(\varphi_{adj} - 1)}$$

All spike bins in which the animal was in the saline zone were multiplied by S_{adj}/S, and spike bins where the animal was in the cocaine zone were multiplied by C_{adj}/C. This had the effect of changing the PYR cocaine index without affecting the firing rate averaged over the entire exploration session.

Sleep replay analysis

For the sleep replay analysis (Figures 4I–4N), we used a Bayesian decoder to estimate the probability of PYR spiking encoding the cocaine or saline zones. To calculate the participation index Ψ, we separated replays into the third of events most likely to encode the saline zone, the third most likely to encode the center zone, and the third most likely to encode the cocaine zone. If Ψ_S is the probability of a neuron firing during a saline zone replay, and Ψ_C is the probability of the neuron firing during a cocaine zone replay, then the participation index $\Psi = \Psi_C - \Psi_S$. $\Delta\Psi$ represents the difference in Ψ between pre-exploration sleep and post-exploration sleep.

The location index L represents the mean location encoded by a replay event in which a given cell fires (saline zone = -1, cocaine zone = 1). ΔL thus represents the difference in L between pre-exploration sleep and post-exploration sleep. The comparison (Figures 4L–4N) between MSNs encoding the saline and cocaine zones is based on MSNs with negative firing rate indices during exploration (saline) versus positive firing rate indices (cocaine). For all replay analyses, cells that fired in fewer than 1% of all sharp wave ripples were omitted from analysis.

Statistical analysis

All analyses and statistical tests were performed using MATLAB (The MathWorks). Most comparisons employed nonparametric Wilcoxon rank sum tests or sign rank tests (for paired statistics). Comparisons of cocaine index were performed using two-tailed t tests for two reasons: 1) cocaine indices are approximately normally distributed, and 2) changes in cocaine index represent changes in a relatively sparse subpopulation of cells that are better captured by the mean of a distribution than the median. Two-way comparisons were performed with either standard two-way ANOVA or mixed model between/within subjects ANOVA when appropriate. Confidence intervals plotted on CDFs represent $\alpha = 0.05$ unless stated otherwise and were derived from bootstrap resampling of the sample distribution with replacement. Data points were excluded if the MSN firing rate was below 0.01 Hz and/or if the GLM failed to converge. When hippocampal activity is a predictor, $\sim$7% of MSNs were excluded by these criteria.

DATA AND SOFTWARE AVAILABILITY

The data and code that support the findings of this study will be made available from the corresponding author upon reasonable request.